



**HAL**  
open science

# Snail hosts abundance mediates the effects of antagonist interactions between trematodes on the transmission of human schistosomes.

Philippe Douchet, Bart Haegeman, Jean-François Allienne, Jérôme Boissier, Bruno Senghor, Olivier Rey

## ► To cite this version:

Philippe Douchet, Bart Haegeman, Jean-François Allienne, Jérôme Boissier, Bruno Senghor, et al.. Snail hosts abundance mediates the effects of antagonist interactions between trematodes on the transmission of human schistosomes.. 2024. hal-04650319

**HAL Id: hal-04650319**

**<https://hal.science/hal-04650319>**

Preprint submitted on 16 Jul 2024

**HAL** is a multi-disciplinary open access archive for the deposit and dissemination of scientific research documents, whether they are published or not. The documents may come from teaching and research institutions in France or abroad, or from public or private research centers.

L'archive ouverte pluridisciplinaire **HAL**, est destinée au dépôt et à la diffusion de documents scientifiques de niveau recherche, publiés ou non, émanant des établissements d'enseignement et de recherche français ou étrangers, des laboratoires publics ou privés.

See discussions, stats, and author profiles for this publication at: <https://www.researchgate.net/publication/379596313>

# Snail hosts abundance mediates the effects of antagonist interactions between trematodes on the transmission of human schistosomes.

Preprint · March 2024

DOI: 10.21203/rs.3.rs-4145796/v1

CITATIONS

0

READS

63

6 authors, including:



**Philippe Douchet**

Université de Perpignan

4 PUBLICATIONS 23 CITATIONS

SEE PROFILE



**J-F Allienne**

Université de Perpignan

116 PUBLICATIONS 2,138 CITATIONS

SEE PROFILE



**Jerome Boissier**

Université de Perpignan

195 PUBLICATIONS 3,616 CITATIONS

SEE PROFILE



**Bruno Senghor**

Institute of Research for Development

33 PUBLICATIONS 595 CITATIONS

SEE PROFILE

# Snail hosts abundance mediates the effects of antagonist interactions between trematodes on the transmission of human schistosomes.

Philippe Douchet

[philippe.douchet@univ-perp.fr](mailto:philippe.douchet@univ-perp.fr)

IHPE: Interactions Hotes-Pathogenes-Environnements <https://orcid.org/0000-0002-6689-1710>

Bart Haegeman

UMR7621: Laboratoire d'Océanographie Microbienne

Jean-François Allienne

IHPE: Interactions Hotes-Pathogenes-Environnements

Jérôme Boissier

IHPE: Interactions Hotes-Pathogenes-Environnements

Bruno Senghor

IRD: Institut de recherche pour le developpement

Olivier Rey

IHPE: Interactions Hotes-Pathogenes-Environnements

---

## Research Article

**Keywords:** Biodiversity, Parasites, Hosts Abundance, Trematodes, Schistosomiasis, Antagonistic Interaction, Transmission

**Posted Date:** April 4th, 2024

**DOI:** <https://doi.org/10.21203/rs.3.rs-4145796/v1>

**License:**   This work is licensed under a Creative Commons Attribution 4.0 International License.

[Read Full License](#)

---

1 Snail hosts abundance mediates the effects of antagonist interactions  
2 between trematodes on the transmission of human schistosomes.

---

3

4 **Philippe Douchet**<sup>1</sup>, **Bart Haegeman**<sup>2</sup>, **Jean-François Allienne**<sup>1</sup>, **Jérôme Boissier**<sup>1</sup>, **Bruno Senghor**<sup>3</sup>,  
5 **Olivier Rey**<sup>1</sup>

6

7 **Contact Informations:**

8 <sup>1</sup> IHPE, Univ Montpellier, CNRS, IFREMER, Univ Perpignan Via Domitia, Montpellier, France

9 <sup>2</sup> CNRS/Sorbonne Université, UMR7621, Laboratoire d'Océanographie Microbienne, Banyuls-surMer,  
10 France

11 <sup>3</sup> IRD, campus UCAD-IRD de Hann, CP 18524, BP 1386 Dakar, Senegal

12

13 **Corresponding author : Olivier Rey** : [olivier.rey@univ-perp.fr](mailto:olivier.rey@univ-perp.fr)

14 **Other co-author : Philippe Douchet** : [philippe.douchet@univ-perp.fr](mailto:philippe.douchet@univ-perp.fr)

15 **Bart Haegeman** : [bart.haegeman@cnr.fr](mailto:bart.haegeman@cnr.fr)

16 **Jean-François Allienne** : [jean-francois.allienne@univ-perp.fr](mailto:jean-francois.allienne@univ-perp.fr)

17 **Jérôme Boissier** : [boissier@univ-perp.fr](mailto:boissier@univ-perp.fr)

18 **Bruno Senghor** : [bruno.senghor@yahoo.fr](mailto:bruno.senghor@yahoo.fr)

19

## 20 **Declarations**

21 This study was a part of a large project investigating the *Schistosoma* invasive capacity (Grant number:  
22 EDCTP-TMA2018CDF-2370-Sen\_Hybrid\_Invasion).

23 **Ethics approval and consent to participate**

24 The project has received approval from the National Ethical Committee (CNERS) of Senegal (agree-  
25 ment number: 00061/MSAS/CNERS/SP).

26 **Consent for publication**

27 “Not applicable”

28 **Availability of data and materials**

29 All data generated or analysed during this study are included in this published article [and its supple-  
30 mentary information files].

31 This project obtained from the Nagoya office in Senegal, an exemption from authorization of access  
32 and use of genetic resources (number: 001339 of November 15, 2021, reference: V/L du 28 octobre  
33 2021) by the Competent National Authority (Directorate of National Parks of Senegal).

34 **Competing interests**

35 The authors declare that they have no competing interests

36 **Funding:**

37 This study was supported in part by the European and Developing Countries Clinical Trials Partnership  
38 (EDCTP2) programme (TMA2018CDF-2370), supported by the European Union. It was funded by the  
39 French Agency for Food, Environmental and Occupational Health & Safety (PNRES 2019/1/059 Molrisk)  
40 and the Occitanie Region (Schistodiag program). It was also supported by the European and Developing  
41 Countries Clinical Trials Partnership (EDCTP2) programme (TMA2018CDF-2370), supported by the  
42 European Union. This study was carried out with the support of LabEx CeMEB, an ANR "Investissements  
43 d'avenir" program (ANR-10- LABX-04-01), and within the framework of the “Laboratoire d'Excellence  
44 (LABEX)” TULIP (ANR-10LABX-41).

45 **Authors' contributions**

46 **PD** have made substantial contributions to the conception, design of the work, acquisition,  
47 analysis, and interpretation of data. He was a major contributor in writing the manuscript, have  
48 approved the submitted version, and have agreed both to be personally accountable for the author's  
49 own contributions and to ensure that questions related to the accuracy or integrity of any part of the

50 work, even ones in which the author was not personally involved, are appropriately investigated,  
51 resolved, and the resolution documented in the literature.

52 **BH** have made substantial contributions to the creation of the mathematical model used in the work,  
53 the analysis, and interpretation of data. He was a major contributor in writing the manuscript, have  
54 approved the submitted version, and have agreed both to be personally accountable for the author's  
55 own contributions and to ensure that questions related to the accuracy or integrity of any part of the  
56 work, even ones in which the author was not personally involved, are appropriately investigated,  
57 resolved, and the resolution documented in the literature.

58 **JFA** have made substantial contributions to the acquisition of the molecular data. He have approved  
59 the submitted version, and have agreed both to be personally accountable for the author's own  
60 contributions and to ensure that questions related to the accuracy or integrity of any part of the work,  
61 even ones in which the author was not personally involved, are appropriately investigated, resolved,  
62 and the resolution documented in the literature.

63 **JB** have made substantial contributions to the conception, design of the work,  
64 acquisition, and interpretation of data. He have approved the submitted version, and have agreed both  
65 to be personally accountable for the author's own contributions and to ensure that questions related  
66 to the accuracy or integrity of any part of the work, even ones in which the author was not personally  
67 involved, are appropriately investigated, resolved, and the resolution documented in the literature.

68 **BS** have made substantial contributions to the acquisition of the field data. He have approved the  
69 submitted version, and have agreed both to be personally accountable for the author's own  
70 contributions and to ensure that questions related to the accuracy or integrity of any part of the work,  
71 even ones in which the author was not personally involved, are appropriately investigated, resolved,  
72 and the resolution documented in the literature.

73 **OR** have made substantial contributions to the conception, design of the work, acquisition,  
74 and interpretation of data. He was a major contributor in writing the manuscript, have approved the  
75 submitted version, and have agreed both to be personally accountable for the author's own

76 contributions and to ensure that questions related to the accuracy or integrity of any part of the work,  
77 even ones in which the author was not personally involved, are appropriately investigated, resolved,  
78 and the resolution documented in the literature.

## 79 **Acknowledgments**

80 The authors warmly thank the Bio-Environnement platform (University of Perpignan Via Domitia) for  
81 sequencing and bioinformatics services. We would like to thank Pr Doudou Sow who allowed us to  
82 process the samples and snail experimental infestations in the laboratory of Parasitology and Mycology  
83 of the Gaston Berger University and EDCTP2 Program supported by the European Union, which  
84 supported our flight and field works in Senegal. Furthermore, we thank Alassane Dit Baye Ndiaye and  
85 Modou Diop for their help in the field.

86

## 87 **Keywords (3 to 10)**

88 **Biodiversity, Parasites, Hosts Abundance, Trematodes, Schistosomiasis, Antagonistic Interaction,**  
89 **Transmission**

90

## 91 [1. Abstract \(350 mots MAX\)](#)

### 92 **Background:**

93 Combating infectious diseases and halting biodiversity loss are intertwined challenges crucial to ensure  
94 global health. Biodiversity can constrain the spread of vector-borne pathogens circulation,  
95 necessitating a deeper understanding of ecological mechanisms underlying this pattern. Our study  
96 evaluates the relative importance of biodiversity and the abundance of *Bulinus truncatus*, a major  
97 intermediate host for the trematode *Schistosoma haematobium* on the circulation of this human  
98 pathogen at aquatic transmission sites.

99 **Methods:** We combined mathematical modelling and a molecular based empirical study to specifically  
100 assess the effect of co-infections between *S. haematobium* and other trematodes within their *B.*

101 *truncatus* snail hosts; and *B. truncatus* abundance at transmission sites, on the production of *S.*  
102 *haematobium* infective cercariae stages released into the aquatic environment.

### 103 **Results:**

104 Our modelling approach shows that more competitive trematode species exploiting *B. truncatus* as an  
105 intermediate host at the transmission site level leads to higher co-infection rates within snail hosts,  
106 subsequently reducing the production of *S. haematobium* cercariae. Conversely, an increase in *B.*  
107 *truncatus* abundance results in lower co-infection rates, and a higher proportion of *S. haematobium*  
108 cercariae released into the environment. Our empirical data from the field support these findings,  
109 indicating a significant negative effect of local trematode species richness and co-infection rates on the  
110 dominance of *S. haematobium*, while *B. truncatus* abundance positively influences *S. haematobium*  
111 dominance.

### 112 **Conclusions:**

113 Our study highlights the importance of biodiversity in influencing the transmission of *S. haematobium*  
114 through the effect of antagonistic interactions between trematodes within bulinid snail hosts. This  
115 effect intensifies when *B. truncatus* populations are low, promoting co-infections within snails. In line  
116 with the need for concrete applications of the One Health concept, we advocate for maintaining high  
117 global freshwater biodiversity to sustain global trematode diversity at transmission sites, offering a  
118 cost-effective means to significantly reduce schistosome prevalence and intensity while preserving  
119 aquatic ecosystem services.

120

121

## 122 2. Introduction

123 One of the major consequences of global change is a drastic modification of the circulation of  
124 pathogens and an increase in disease emergences and outbreaks worldwide (1–3). The causes of these  
125 global-scale increases are multifactorial and the profound changes in biodiversity observed globally  
126 contribute significantly (4). On one hand, while some populations/species are extending, including



127 humans and all domesticated species upon which human societies rely, most populations of most  
128 species are declining (5,6). On the other hand, it is generally assumed that parasite transmission  
129 increases with host density although generally not linearly (7). As a result, the growth and densification  
130 of human populations and domestic organisms contribute to the emergence and circulation of  
131 numerous pathogens sometimes causing severe health and economic issues which tend to extend at a  
132 planetary scale due to global international trades (8). Moreover, the reduction in biodiversity in an  
133 existing community of hosts and parasites can lead to a decrease in the abundance of non-competent  
134 hosts, which, when present, mitigate the circulation of parasites through a dilution effect (9). The  
135 generality and ecological importance of this dilution effect is however widely debated (10–12).  
136 Additionally, host diversity in a community can support the co-existence of several circulating pathogen  
137 species, between which antagonistic (or beneficial) interactions within their hosts or vectors can  
138 significantly hamper (or facilitate) the circulation of least competitive pathogens (13).

139 Both facilitating and antagonistic interactions exist between trematodes. These parasitic  
140 worms display complex life cycles more generally including a vertebrate organism as definitive hosts  
141 and several successive invertebrate and/or vertebrate organisms are intermediate hosts including most  
142 of the time (aquatic) snails as first intermediate hosts. Such complex life cycles provide opportunities  
143 for interactions between trematode species and modulation of their transmission dynamics when  
144 coinfection occur especially in snail species that generally serve as amplifiers of trematodes in the  
145 environment. Some trematodes are causative agents of severe forms of Human and livestock diseases  
146 such as *Schistosoma* species. Interactions between *Schistosoma* species and other trematodes were  
147 historically documented with a focus on antagonistic interactions that could hamper their transmission  
148 as a mean of potential biological control strategies (14).

149 In fact, accruing evidence suggest that *Schistosoma* species that develop into sporocysts within their  
150 snail hosts are considered as moderate to bad competitors compared to other trematode species (13).  
151 Moreover, other trematode species that develop into rediae within snail hosts can predate the co-  
152 occurring *Schistosoma* sporocysts under development while consuming snail tissues (15). At natural

153 transmission sites of *Schistosoma* species, the importance of such antagonist interactions on the  
154 circulation of *Schistosoma* species is generally underappreciated. Importantly however the snail  
155 intermediate hosts used by some *Schistosoma* species (e.g. *Biomphalaria* spp., *Bulinus* spp.) generally  
156 host numerous trematode species hence providing opportunities for many intra-host interactions that  
157 involve *Schistosoma* species. For example, up to 29 trematode species have been identified in natural  
158 populations of *Biomphalaria pfeifferi* and *Biomphalaria sudanica* established over a constrained  
159 geographical scale, these two snail species being important hosts for *Schistosoma mansoni* in eastern  
160 Africa (13). Moreover, and as previously mentioned, *Schistosoma* species harbor low competitiveness  
161 compared to many other species of trematodes (13). In line with these two characteristics, recent  
162 modelling approaches predict over 50% decrease in the transmission of *S. mansoni* in the presence of  
163 some highly competitive trematodes coinfecting *B. pfeifferi* – such as *Calicophoron sukari*, a widely  
164 distributed parasite across livestock (13).

165         As a simple baseline, the prevalence of coinfection in a host population harbouring two  
166 parasites equals the product of the prevalence of single infection of each parasite in the population  
167 (15). However, coinfection rates observed *in natura* are generally lower than this theoretical  
168 expectation. Interspecific competition leading to the rapid exclusion of one interacting species,  
169 recruitment heterogeneity either due to random or parasite behaviours that limit co-infections,  
170 immune priming mechanisms and high cost of co-infection on hosts fitness, may explain the departure  
171 of this theoretical expectation as generally observed *in natura* (15,16). Intriguingly, the effect of host  
172 abundance on co-infection rates is generally neglected since this theoretical expectation relies on the  
173 relative prevalence of co-infection, which corresponds to the proportion of hosts that are infected (or  
174 co-infected) among all hosts present in the environment. However, according to the generally  
175 acknowledged density-dependent nature of pathogen transmission, it is expected that host density  
176 also influences the co-infection rates, the occurrence of antagonistic interactions and ultimately the  
177 transmission of less competitive parasites. If so, this could constitute an additional indirect mechanism

178 by which host density is positively correlated with parasite transmission by reducing co-infections and  
179 a release from antagonistic interactions.

180           Using the *Schistosoma haematobium* – *Bulinus truncatus* system as a model, the objective of  
181 this study is to assess the relative importance of the density of *B. truncatus* at transmission sites and  
182 the diversity of trematodes that use *B. truncatus* on the risk of transmission of *S. haematobium*.  
183 *Schistosoma haematobium* is a trematode species causing the urogenital form of bilharziasis in Humans  
184 mainly in the tropical regions in Africa (17). It displays a complex two-host lifecycle that involves  
185 humans as vertebrate hosts, in which the adults develop and reproduce sexually resulting in the  
186 production of thousands of eggs that are released in the environment through the urinary system of  
187 the host; and *Bulinus truncatus*, a freshwater snail host in which the parasite reproduce asexually  
188 resulting in the production of cercariae that are released in the aquatic environment and actively seek  
189 and penetrate the skin of a new vertebrate definitive host.

190           We hypothesise that for a given abundance of *B. truncatus*, an increase in the specific richness  
191 of trematodes using *B. truncatus* as a host at the community scale would lead to an increase in co-  
192 infection rates that involves *S. haematobium*. Given that *Schistosoma* species (including *S.*  
193 *haematobium*) tend to be moderate competitors, an increase in the rate of co-infection is expected to  
194 reduce the development of *S. haematobium* within their snail hosts and so the total amount of *S.*  
195 *haematobium* cercariae released from the snails into the aquatic environment and ultimately the risk  
196 of transmission to their definitive hosts. Moreover, an increase in the abundance of *B. truncatus* would  
197 lead to a reduction of the co-infection rates and the associated antagonistic interactions thus ultimately  
198 enhancing the risks of schistosomiasis transmission to Humans.

199           To test these hypotheses, we first built a simple mathematical model to describe (i) how the  
200 number of competitive trematodes using *B. truncatus* influence the amount of *S. haematobium*  
201 cercariae released in aquatic systems and (ii) how snail density (here carrying capacity) influences co-  
202 infections rates and the associated antagonistic effects on the release of *S. haematobium* cercariae at  
203 the transmission site level. We confronted this mathematical model to an empirical field work study

204 conducted in Northern Senegal at 9 previously identified urogenital schistosomiasis transmission sites.  
 205 We combined traditional malacological and parasitological approaches and next-generation molecular  
 206 tools to empirically study the effect of the trematodofauna using *B. truncatus* as intermediate host and  
 207 the local abundance of *B. truncatus* on the transmission of *S. haematobium*.

208

209

### 210 3. Material and methods

#### 211 3.1. Mathematical model

##### 212 2.1.1. Model with one trematode species

213 We start by modelling the infection of a snail population by a single trematode species. The  
 214 model tracks the dynamics of the density of miracidia, susceptible and infected snails, and cercariae in  
 215 the aquatic ecosystem, denoted by the variable  $M(t)$ ,  $S(t)$ ,  $I(t)$  and  $C(t)$  respectively. The dynamics are  
 216 described by the following set of ordinary differential equation :

$$\begin{aligned}\frac{dM}{dt} &= g - eSM - d_M M \\ \frac{dS}{dt} &= -eSM - d_S S + f_S S \left(1 - \frac{S+I}{K}\right) \\ \frac{dI}{dt} &= eSM - d_I I + f_I I \left(1 - \frac{S+I}{K}\right) \\ \frac{dC}{dt} &= sI - d_C C - uC\end{aligned}$$

217 These equations use the following parameters:  $g$  : input rate of miracidia;  $e$  : infection rate of  
 218 susceptible snails by miracidia ;  $f_S, f_I$  : fitness of susceptible and infected snails;  $K$  : carrying capacity of  
 219 snail population;  $s$  : shedding rate of infected snails;  $u$  : uptake rate of cercariae by mammals;  $d_M, d_S, d_I$   
 220 ,  $d_C$  : loss rates of miracidia, susceptible snails, infected snails, cercariae. Because infection reduces  
 221 fitness and increases mortality,  $f_I < f_S$  and  $d_I > d_S$ . For simplicity we set  $f_I = 0$  and  $d_S = 0$ . Note that the  
 222 model does not describe the complete trematode life cycle. Rather, the model starts from a given  
 223 exposure to miracidia (parameter  $g$ ) and predicts the cercariae density (variable  $C$ ), or equivalently the  
 224 uptake of cercariae by mammal hosts (equal to  $uC$ ). To simplify the study of the model, we look at its  
 225 equilibrium properties (Additional \_File\_1\_(Figure\_S1)).

226

227 *2.1.2. Model with two trematode species*

228 Next, we consider two trematode species infecting a snail population. We call these two species

229 1 and 2. Compared to the previous model, we extend the list of variables as follows: miracidia  $M_1$  and

230  $M_2$ , susceptible  $S$ , infected  $I_1$ ,  $I_2$  and co-infected  $I_{12}$ , and cercariae  $C_1$  and  $C_2$ . The equations are :

$$\begin{aligned}\frac{dM_1}{dt} &= g_1 - e_1SM_1 - d_{M_1}M_1 \\ \frac{dM_2}{dt} &= g_2 - e_2SM_2 - d_{M_2}M_2 \\ \frac{dS}{dt} &= -e_1SM_1 - e_2SM_2 + f_S S \left(1 - \frac{S + \sum I}{K}\right) \\ \frac{dI_1}{dt} &= e_1SM_1 - e_2I_1M_2 - d_{I_1}I_1 \\ \frac{dI_2}{dt} &= e_2SM_2 - e_1I_2M_1 - d_{I_2}I_2 \\ \frac{dI_{12}}{dt} &= e_2I_1M_2 + e_1I_2M_1 - d_{I_{12}}I_{12} \\ \frac{dC_1}{dt} &= s_1I_1 + s_{1|2}I_{12} - d_{C_1}C_1 - u_1C_1 \\ \frac{dC_2}{dt} &= s_2I_2 + s_{2|1}I_{12} - d_{C_2}C_2 - u_2C_2\end{aligned}$$

231 The meaning of the model parameters is as before, but now with the indices 1 and 2 referring to the

232 trematode species. For the shedding rates,  $s_1$  is the shedding rate of cercariae of species 1 by a snail

233 infected by species 1 only, whereas  $s_{1|2}$  is the shedding rate of cercariae of species 1 by a snail infected

234 by both species. Similar definitions hold for  $s_2$  and  $s_{2|1}$ . We assume that the two trematode species only

235 differ in their shedding rates. The term “shedding” used in the model reflect the transition from the

236 day when snails become infected to the release of cercariae, and hence also includes the development

237 of the trematodes within the snail hosts. Taking species 1 as a *Schistosoma* species, we model its

238 inferior competitiveness by taking  $s_{1|2} < s_{2|1}$  (i.e., co-infected snails preferentially shed cercariae of species

239 2). For simplicity, we set  $s_{1|2} = 0$  and  $s_{2|1} = s_2$ . In other words, snails that are infected by both species do

240 not shed *Schistosoma* cercariae, and they shed cercariae of the other species at the same rate as a snail

241 not co-infected by *Schistosoma*. Apart from this difference in shedding rates, we assume the two

242 trematode species to be equivalent for all other model parameters (Additional

243 \_File\_2\_&\_3\_(Figure\_S2\_and\_S3)).

244

245 *2.1.3. Model with multiple trematode species*

246 The above model can be extended to more than two trematode species. We denote by  $n$  the  
247 number of trematode species, and assume that snails can be infected by one, two, . . . , all  $n$  species.  
248 We make the same assumptions as above, that is, all trematode species are assumed to be equivalent  
249 apart from their shedding rates. In particular, we consider one *Schistosoma* species and  $n-1$  other  
250 trematode species and assume that there is no shedding of *Schistosoma* cercariae in case snails are co-  
251 infected with (one or more) other trematode species. We assume that the miracidia input rate per  
252 trematode species is independent of diversity, so that the total input rate (i.e., summed over all  
253 trematode species) increases proportionally with diversity. In particular, the input rate of *Schistosoma*  
254 miracidia is unaffected by the presence of other trematode species. We assume that the total shedding  
255 rate (i.e., the shedding rate per infected snail and summed over all shedded trematode species) is  
256 independent of the number of species infecting the snail. This implies that the shedding rate per snail  
257 infected by a particular trematode species decreases with trematode diversity, as some of these snails  
258 are co-infected with other trematode species. This holds especially for snails infected by *Schistosoma*,  
259 as co-infection by another trematode species causes the *Schistosoma* shedding rate to drop to zero. An  
260 additional file provides an in-depth description of the model equations and our simulations  
261 (Additional\_File\_4\_(Supplementary\_material), Additional\_File\_5\_&\_6)

262

263 3.2. Empirical field work

264 *2.2.1. Study sites description and ethical consideration*

265 An empirical fieldwork study was carried out in the region of the Senegal river basin during the  
266 dry season in February 2022 (Figure 1). We targeted 9 previously identified *S. haematobium*  
267 transmission sites that differ from an ecological point of view (i.e. river, irrigation canal and lake) and  
268 hence possibly harbouring different trematode communities. Each of these transmission sites is close  
269 to a village where the prevalence and intensity of urogenital schistosomiasis among children was  
270 previously reported (18).

271 The transmission sites close to the villages of Ndiawara (16°35'04"N / 14°50'58"W), Ouali Diala  
272 (16°35'56"N / 14°56'10"W), Dioundou (16°35'50"N / 14°53'22"W), Fonde Ass (16°36'20"N /  
273 14°57'38"W) and Khodit (16°35'45"N / 14°56'42"W) are located in the middle valley along a tributary  
274 of the Senegal River ("le Doue" river). The transmission site close to the village of Guia (16°35'51"N /  
275 14°55'31"W) is located along an irrigation canal that drains water from the river "le Doue". The  
276 transmission sites nearby the villages of Mbane (16°16'15"N / 15°48'7"W) and Saneinte (16°14'32"N /  
277 15°48'6"W) are located along the east shore of the lake de Guiers. The transmission site close to the  
278 village of Lampsar (16°6'34"N / 16°20'58"W) is in an inlet in the lower valley of the Senegal river delta  
279 (Figure 1).

280

#### 281 *2.2.2. eDNA, snails and trematodes field sampling*

282 To assess the abundance of *B. truncatus* and to identify all trematode species present at each  
283 of the 9 studied sites as free-living stages, aquatic environmental DNA samples (eDNA) were collected  
284 using water filter capsules according to Douchet et al. (2022). Filtrations were carried out from the  
285 entire water column along the banks until the filter's membrane clogged, and the volume filtered at  
286 each site was recorded. At each site but Khodit, 1.5L of commercial spring water was filtered following  
287 the same protocol as a technical field negative control. Once the water filtrations completed, capsules  
288 were drained, filled with 50 mL of Longmire buffer solution to preserve eDNAs, vigorously shaken, and  
289 stored at room temperature and at dark until subsequent DNA extraction.

290 Once the eDNA sampling achieved, all snails found at each sampling site were systematically  
291 collected manually or by scooping the grass on the water bench using a colander for about 30 minutes  
292 to one hour. Snails were morphologically identified and individualized on well plates filled with  
293 dechlorinated water and left to emit trematodes for 2 h in the afternoon under natural sunlight.  
294 Cercariae from each emitting snail were collected and transferred onto FTA cards and stored at room  
295 temperature until DNA extraction and molecular identification. Coupled with eDNA samples, this  
296 approach allows a better characterisation of the trematode community at each transmission site and a

297 quantification of the prevalence of each emitted trematode species among the locally established snail  
298 populations including *Bulinus truncatus*. All snails morphologically identified as *B. truncatus* (either  
299 emitting or non-emitting) were preserved individually in alcohol until DNA extraction. Subsequent  
300 molecular analyses aimed at validating the species attribution of each *B. truncatus* individual, check for  
301 the presence and identification of potentially developing trematodes within each snail, refine measures  
302 of prevalence of each trematode species, and identify possible coinfections.

303

### 304 3.3. Experimental infection

305 Twenty six non-emitting snails (although possibly naturally infected by trematodes) sampled at  
306 sites Guia, Fonde Ass, Khodit and Saneinte were kept alive and individually exposed to 3 *S.*  
307 *haematobium* miracidia for 2 hours in 24 well plates filled with dechlorinated water. The miracidia used  
308 for this experimental mollusc exposition were from a homogenised pool of *S. haematobium* eggs of  
309 eight children from the Lampsar village provided by the Sen\_Hybrid\_Invasion project. The 104 exposed  
310 snails (i.e. 26 x 4) were maintained and fed *ad libitum* for a period of 1 month and survival was checked  
311 daily. At the end of this period, the infection status of each *B. truncatus* was monitored by emission of  
312 cercariae once a week until the snails died. To this end, *B. truncatus* were individualized on clean well  
313 plates filled with dechlorinated water and stimulated to emit trematodes for 4 h in the afternoon under  
314 artificial light. Cercariae released from emitting snails were collected and stored at -20°C until DNA  
315 extraction for subsequent molecular identification. All along the experiment, each emitting snail was  
316 kept individualised to identify possible trematode species emission shifts through time. At the end of  
317 the experiment, all *B. truncatus* individuals (either emitting or non-emitting) were preserved in alcohol  
318 individually until DNA extraction.

319



### 320 3.4. Molecular approaches

#### 321 2.4.1. DNA extractions from samples

322 To extract eDNAs from water filtrates, the Longmire solution contained in each capsule was  
323 poured into three 50 ml Falcon tubes as technical replicates. For the field negative controls (i.e. Spring  
324 water filtrates), each capsule content was recovered in one 50 ml Falcon tube only. All Falcon tubes  
325 were centrifugated at 16,000 g for 20 min and the supernatant was removed. We then collected 0.25  
326 g to 0.5 g of sediment from the pellet from each falcon tube or 500 µL of Longmire remaining at the  
327 base of the falcon tube when not enough material was observed. For negative controls, 500 µl of  
328 Longmire were systematically retained when discarding the supernatant. This pre-extraction step led  
329 to the processing of 35 samples (i.e., 8 negative controls and 3 extraction replicates for each of the 9  
330 environmental samples). Total environmental genomic DNA was extracted from each triplicate and  
331 negative controls using the Qiagen's Dneasy PowerSoil Pro Kit following supplier recommendation  
332 performing the physical lysis with a MagNA Lyser at a speed of 7,000 for 30s.

333 DNAs from all cercariae obtained from the field survey, from the exposure experiment and from  
334 all *B. truncatus* snails were extracted using the Qiagen DNeasy Blood & Tissue kit. Regarding cercariae  
335 preserved onto FTA cards, we manually isolated 0.5 cm in diameter pieces containing the biological  
336 material using a sterile punch and placed them in 1.5 ml tubes. Four samples consisting in 0.5 cm in  
337 diameter pieces from cards on which ultrapure water had been deposited were also isolated as DNA  
338 extraction negative controls. For cercariae preserved in 1.5 ml tubes stored at -20°C, we thawed the  
339 tubes and centrifuged them at 20,000g for 10 minutes before removing the supernatant. To obtain  
340 extraction and PCR negative controls, we also centrifuged 2 tubes that contained ultrapure water  
341 following the same protocol. For *B. truncatus*, we first rinsed the snails with tap water and ground them  
342 entirely and individually with a sterile pestle in 1.5 mL tubes. To obtain extraction and PCR negative  
343 controls, we also processed 7 assuredly non-infected *B. truncatus* from our laboratory collections in  
344 the same way. Moreover, 3 extraction/PCR positive controls were prepared from 3 additional non-  
345 infected laboratory *B. truncatus* individuals, to which one *S. haematobium* cercariae from our

346 laboratory collections was artificially added before DNA extraction processing. These pre-extraction  
347 steps led to the processing of 328 samples and 16 controls (i.e., 29 FTA card pieces and 4 associated  
348 negative controls, 28 cercaria preserved in alcohol and 2 associated negative controls and 281 *B.*  
349 *truncatus* including 173 *B. truncatus* from the field and 98 from the experimental infection and 3 and  
350 7 associated positive and negative controls). From these samples, we then followed the Tissue protocol  
351 as recommended by the supplier applying a 2 h lysis for cercariae and an overnight lysis for snails.

352

#### 353 *2.4.2. Taxonomical assignment of trematode cercariae by barcoding*

354 To taxonomically assign each cercariae emitted from snail hosts to a trematode species, DNAs  
355 extracted from cercariae of each emitting snail were SANGER sequenced at the 28S D2 rDNA gene  
356 domain and at the 16S rDNA gene (19). PCRs were run using the obtained 57 DNAs extracted from  
357 cercariae and the 6 negative controls on both markers. PCRs were performed using the GoTaq® G2 Hot  
358 Start Polymerase kit of Promega. Each PCR reaction contained Colorless Buffer at 1×, MgCL2 at 1.5 mM,  
359 dNTPs at 0.2 mM, primers at 0.4 μM, 1.25 units of GoTaq G2 Hot Start, 2 μl of DNA sample, and  
360 ultrapure water for a total PCR reaction volume of 35 μL. For the 28S marker, the PCR program was  
361 used as follows: An initial denaturation step at 94°C for 3' followed by 40 cycles with a denaturation  
362 step at 95°C for 30 s, a hybridization step at 56°C for 30 s and an elongation step at 72°C for 30 s. We  
363 finally performed a final elongation step at 72°C for 5'. For the 16S marker, the same PCR program was  
364 used, except that 35 cycles were performed, the hybridization temperature was 54°C and the  
365 elongation time was 15 s. Ten microliters of the resulting PCR products were migrated on a 2% agarose  
366 gel for 20' at 135 V and revealed using a Vilber Infinity 1000 imaging system. Each individual PCR  
367 product from the 57 cercariae DNA extracts that displayed an expected theoretical size was then  
368 sequenced in both the forward and reverse directions on an ABI 3730xl sequencer at the GenoScreen  
369 platform (Lille, France). The sequences generated were aligned, trimmed, and taxonomically assigned  
370 with a MEGABLAST analysis for the 28S and the 16S markers. For the taxonomical assignment of each

371 cercariae, the common taxonomic rank to all hits above 96% of identity over 97% of coverage were  
372 kept.

373

#### 374 *2.4.3. Molecular taxonomic validation of B. truncatus and infection diagnostic*

375 The 271 *Bulinus* spp. sampled in the field from which total DNA was extracted were diagnosed  
376 to verify that they belonged to the species *B. truncatus* using a molecular diagnosis by LAMP based on  
377 the internal transcribed spacer (ITS2) *B. truncatus* species-specific (20). DNAs extracted from *Bulinus*  
378 spp. were first diluted at 1/100e and a negative control consisting in a 1/100e diluted DNA extraction  
379 from *Bulinus globosus* was used. Each LAMP reaction contained an Isothermal Amplification Buffer II  
380 reaction buffer [20 mM Tris-HCl, 10 mM (NH<sub>4</sub>)<sub>2</sub>SO<sub>4</sub>, 150 mM KCl, 2 mM MgSO<sub>4</sub>, 0.1% Tween 20, pH  
381 8.8 at 25 °C (New England Biolabs, UK)] at 1X, additional MgSO<sub>4</sub> at 3 mM, dNTP at 1.0 mM, internal  
382 primers FIP and BIP at 1.2 μM, external primers F3 and B3 at 0.2 μM, LOOP primers LB and LF at 0.4  
383 μM, 1 U of Bst 2.0 WarmStart DNA polymerase (New England Biolabs, UK), 1 μl of DNA sample, and  
384 ultrapure water for a total reaction volume of 10 μL as described in Blin et al., 2023. Reaction were  
385 performed in a thermocycler at 63 °C for 45 min followed by an enzyme inactivation phase at 80 °C for  
386 5 min. Result visualizations were done using a final point visual detection of fluorescence after adding  
387 1 μl of 1:50 diluted 10,000× concentration of SYBR Green (Invitrogen) (green: positive=*B. truncatus*  
388 species; orange: negative=other than *Bulinus* species).

389 To detect trematodes within the tissues of each *B. truncatus*, we used the 16S rDNA gene  
390 metabarcode initially developed to characterize trematode communities from eDNA (19) as a  
391 molecular diagnostic tool. PCRs were performed using the GoTaq® G2 Hot Start Polymerase kit of  
392 Promega following the same PCR condition as described previously [see section 2.4.2], except that  
393 reactions were performed in a final volume of 10 μl and using 2 μL of DNA extracted from *Bulinus* spp.  
394 diluted 1:100. Amplification success was assessed visually by migrating the ten microliters of the  
395 resulting PCR products on a 2% agarose gel for 20' at 135 V and revealed using a Vilber Infinity 1000  
396 imaging system.

397

398 *2.4.4. Trematodes-specific MiSeq sequencing on the infected B. truncatus individuals and on the*  
399 *eDNA to characterize trematode communities*

400 A total of 137 positive 16S metabarcoding NGS libraries were prepared following the Illumina  
401 two-step PCR protocol, using the Trem\_16S\_F1 and the Trem\_16S\_R2 primers set up with Illumina  
402 adapters using 2 µL of eDNA or DNA extracted from *B. truncatus* diluted at 1:100e as previously  
403 described (19). Libraries were sent and paired-end sequenced (2 × 250 bp) on an Illumina MiSeq™ at  
404 the BioEnvironnement platform (University of Perpignan Via Domitia, France). Three samples were  
405 eliminated from the analyses of the MiSeq sequencing because they did not meet the defined  
406 threshold of 25,000 sequences required to normalise samples by rarefaction (i.e., one non emitting  
407 *B. truncatus* from the site Ouali Diala, and two PCR duplicates from water eDNA).

408

409 *2.4.5. Abundance of B. truncatus determination by ddPCR on eDNA*

410 Abundance of *B. truncatus* at each study site was assessed by digital droplet PCR (ddPCR) from  
411 eDNA sampled by water filtration according to (21). We first pooled the eDNA extraction triplicates  
412 from each of the 9 sampling sites. As negative control, we also pooled DNAs extracts from one  
413 individual of each mollusc species sampled during the field work in addition to DNAs extracts from 3 *B.*  
414 *truncatus* sister species (i.e., *B. globosus*, *B. senegalensis* and *B. umbilicatus*) from our laboratory  
415 collection. As positive control, we used a DNA extract at 0.01 ng/µL from one *B. truncatus* from our  
416 laboratory collection. We ran ddPCRs using the TaqMan technology on a QX200 AutoDG Droplet Digital  
417 System (BioRad) at the Bio-environnement platform (Perpignan, France). We used the Btco2F (5'  
418 ATTTTGACTTTTACCACCAT 3') and Btco2R (5' GATATCCCAGCTAAATGAAG 3') primers combined with the  
419 FAM-labelled probe Btco2P (5' TCGAAGGAGGGGTTGGAACAGG-FAM 3'). ddPCR reactions were  
420 performed using the BioRad ddPCR Supermix for Probes (No dUTP). Each ddPCR reaction contained the  
421 BioRad MIX at 1X, primers at 0.5 µM, probes at 0.25 µM, 7 µL of eDNA template or 2 µL of control DNAs  
422 templates, and ultrapure water for a total ddPCR reaction volume of 20 µL. After the droplets

423 generation, the ddPCR program was used as follows: An enzyme activation step at 95°C for 10 min  
424 followed by 40 cycles with a denaturation step at 94°C for 30s and an annealing/extension step at 60°C  
425 for 60s, with a ramp setting to 2°C/s. We finally performed an enzyme deactivation step at 98°C for 10'.  
426 The resulting fluorescence signal were analysed using QuantaSoft software V1.7 (BioRad). A signal was  
427 considered positive (i.e., with the presence of *B. truncatus* DNA) if at least one positive droplet was  
428 detected and if the positive droplet displayed the same order of fluorescence magnitude as the positive  
429 droplet obtained from a ddPCR positive control.

430

### 431 3.5. Data analysis

#### 432 2.5.1. Characterisation of trematode communities present in the water and exploiting *B.*

##### 433 *truncatus* populations

434 The resulting amplicon sequence datasets from the MiSeq sequencing was processed using the  
435 Find Rapidly OTUs with Galaxy Solution (FROGS) (22) according to (19). Briefly, the produced datasets  
436 were pre-processed by filtering out the sequences to keep amplicon sizes from 150 to 400 nucleotides.  
437 The remaining sequences were next clustered into operational taxonomic units (OTUs) using the swarm  
438 algorithm and using denoising and an aggregation distance of three (23). The resulting dataset was  
439 filtered out for chimeras using VSEARCH (24). Singletons and underrepresented clusters (i.e., clusters  
440 whose number of sequences were <0.1% of the total number of sequences) were removed. Lastly, we  
441 conservatively considered that a given OTU was present in a library if its number of sequences was  
442 >0.1% of the total number of sequences in this library.

443 Each OTU was next assigned to a taxonomic level (either a species or a genus) using a two-step  
444 BLAST affiliation process. The first BLAST analysis was computed using the standalone blastn program  
445 contained in the *BLAST+* package and a custom trematode sequence database containing 174  
446 sequences (82 sequences from the NCBI database and 92 sequences from a custom internal trematode  
447 sequence database including the sequences obtained from the amplicons generated by the SANGER  
448 sequencing on cercariae, see section 1.1.7). The second BLAST analysis was performed using the online

449 MEGABLAST tool and based on the nr database without restricting parameters to achieve affiliation of  
450 OTUs that could not be assigned in the first BLAST analysis. OTUs were assigned to a species if the  
451 sequences presented a minimal blast coverage of 97% and a pairwise identity above 99% with the  
452 affiliated sequence. OTUs were assigned to a genus if the sequences presented a minimal blast  
453 coverage of 97% and a pairwise identity above 96% with the affiliated sequence. OTUs that could not  
454 be assigned to a species or genus were assigned to a higher taxonomic rank using a clustering method  
455 based on the pairwise genetic distances between the OTUs and the same set of 174 sequences as  
456 above. We then aligned these sequences with T-Coffee on EMBL-EBI (25) and built a neighbor joining  
457 phenetic tree based on the percentage of nucleotide differences from the obtained alignment using  
458 Jalview version 2.11.1.4 (26) for visualization.

459 Subsequent analyses were then performed on R version 4.3.1. Each library was normalized by  
460 rarefaction at 25,000 reads using the package *Vegan* version 2.6-4. The trematode composition, specific  
461 richness and relative abundance in each *B. truncatus* individual or water sample was next assessed  
462 using the package *phyloseq* (27). We assessed the co-infection rates among infected *B. truncatus* and  
463 the number of trematode species involved in each co-infection. We also tested whether parasite  
464 aggregation at the *B. truncatus* individual scale occurred by comparing the observed distribution of  
465 trematode species within hosts with a theoretical distribution following a negative binomial  
466 distribution using a Chi-square test.

467

#### 468 *2.5.2. Abundance of B. truncatus at each sampling site*

469 The *B. truncatus* eDNA copy number per liter of filtered water ( $C_L$ ) estimated from the ddPCR  
470 results was used as a proxy of the abundance of *B. truncatus* at each sampling site.  $C_L$  was calculated  
471 from the following equation (21):

$$472 \quad C_L = \frac{\frac{C_{rdd} * V_e}{V_r}}{V_w}$$

473 With  $C_L$ : the number of eDNA c/L for the amplified sample ;  $C_{dd}$ : the copy number per reaction  
474 volume ;  $V_e$ : the total volume of eluted DNA after extraction ;  $V_r$ : the volume of extracted DNA used for  
475 ddPCR reaction ; and  $V_w$ : the total volume of filtered water.

476

477 *2.5.3. Assessing the link between the relative abundance of Schistosoma quantified in co-*

478 *infected B. truncatus and the emission status of Schistosoma cercariae by co-infected B.*

479 *truncatus*

480 To determine whether the dominance status of *Schistosoma* species in terms of percentage of  
481 reads of these species within *B. truncatus* individuals co-infected with other trematode species can be  
482 used as a proxy of *Schistosoma* cercarial release, we performed a generalised linear model (GLM) using  
483 the package *stats* version 4.3.1 implemented in R. A subset from our dataset that contained 14 *B.*  
484 *truncatus* individuals from the field work and from the experimental infection were used for this  
485 analysis. These individuals were all emitters, co-infected and harboured at least *S. haematobium* or *S.*  
486 *bovis*. We set the emission status (i.e. 0 and 1: non-emitting and emitting *Schistosoma* sp.) as the  
487 dependent variable and the relative abundance of the respective *Schistosoma* species in terms of  
488 percentage of sequences compared to the other co-infecting trematode species as explanatory  
489 variable. The model was built assuming a quasibinomial distribution of the data.

490

491 *2.5.4. Effect of trematode species richness, co-infection rates and host abundance on the*

492 *average dominance of schistosomes*

493 To test our initial hypotheses, we ran three independent generalized linear mixed models  
494 (GLMM) using the package *lme4* version 1.1-33 implemented in R to infer the effect of (i) the overall  
495 trematode species richness using *B. truncatus* as an intermediate host at the population level, (ii) the  
496 co-infection rate among the infected *B. truncatus* snails, and (iii) the abundance of *B. truncatus*; on the  
497 average dominance of schistosomes within host populations (i.e., the relative abundance of *S.*  
498 *haematobium* or *S. bovis* in terms of percentage of sequences compared to the other co-infecting

499 trematode species). Only naturally infected *B. truncatus* from the field were considered in this analysis,  
500 excluding *B. truncatus* from the experimental infection. To account for pseudo-replication, we set the  
501 sampling site as a random factor. For these analyses, the co-infection rate variable was transformed  
502 into two categories (i.e. <50% and >50% co-infection among infected individuals). The *B. truncatus*  
503 abundance variable was also transformed into two categories (i.e. <200 and >200  $C_L$ ) to compare sites  
504 at low and medium to high density according to Mulero et al. 2020. The variable “trematode species  
505 richness” (that uses *B. truncatus*) was coded as the number of trematode species other than  
506 *Schistosoma* which use local *B. truncatus* population at the site level. We assumed a binomial error  
507 term in the three models tested.

508

509

## 510 4. Results

### 511 4.1. Mathematical model

512 Our mathematical model indicates that, for a fixed carrying capacity of *B. truncatus* (either  
513 small or large), a local increase in the number of competitive trematode species using *B. truncatus* as  
514 intermediate host leads to an increase in the co-infection rate within individual snails and ultimately to  
515 a decrease in the number of *S. haematobium* cercariae produced (Figure 2). Moreover, an increase of  
516 carrying capacity of *B. truncatus* leads to a decrease of the proportion of co-infected snails and an  
517 increase in the proportion of *Schistosoma* cercariae (Figure 2). In other words, an increase in the  
518 number of competitive trematode species using *B. truncatus* as intermediate host can reduce the  
519 production of *S. haematobium* cercariae through antagonist interactions and particularly so when *B.*  
520 *truncatus* populations are small. An increase in *B. truncatus* populations mitigates the effect of  
521 antagonist interactions by reducing the coinfection rate among snail hosts.

522



#### 523 4.2. Empirical field study

524 Except *Bulinus forskalii* that was recorded at low abundance at 3 sites (i.e., Ouali Diala, Guia  
525 and Khodit), *B. truncatus* was the only *Bulinus* species found during the field survey. The species  
526 identity of the 271 snails initially identified as *B. truncatus* based on their morphology, and from which  
527 total DNA was extracted, was validated by the LAMP-based diagnostic tool. The abundance of *B.*  
528 *truncatus* among sites assessed based on digital PCRs results varied from 41 to 2176 eDNA copies per  
529 litre filtered (Table 1).

530 In addition to *S. haematobium* and its sister species *S. bovis*, we identified 9 trematode species  
531 associated with *B. truncatus* populations. Nine trematode species were sampled during our fieldwork  
532 (Figure 3), and two additional trematode species were detected during the monitoring of  
533 experimentally infected *B. truncatus* individuals, including *Apharyngostrigea pipientis* and an  
534 *Echinostoma* species that we could not determine at the species level (Additional\_File\_7\_(Table S1)).  
535 An additional species (i.e. Paramphistomoidea sp. 3) was found associated to two *B. truncatus*  
536 individuals from the experimental infection (Additional\_File\_7\_(Table S1)) under the appearance of  
537 cysts attached on their shell (despite washing) but with no apparent shedding from snails. The number  
538 of trematode species other than *S. haematobium* and *S. bovis* using the *B. truncatus* population at each  
539 site varied from 0 to 4 species and the co-infection rates among infected individuals from 0 to 100%  
540 (Figure 3; Table 1). The distribution of the number of trematode species per *B. truncatus* individual  
541 from the field did not differ significantly from a theoretical negative binomial distribution hence  
542 indicating a classical parasite aggregation pattern in *B. truncatus* populations  
543 (Additional\_File\_8\_(Figure S4)).

544 Apart from the *B. truncatus* population, a total of 20 trematode species were detected from  
545 the water samples, 7 of which were also detected in *B. truncatus* while 2 trematodes detected in *B.*  
546 *truncatus* were not detected from the water samples. *Schistosoma haematobium* and/or *S. bovis* were  
547 detected from eDNA water filtrates at 5 among the 9 targeted sites (Additional\_File\_9\_(Table S2)).

548

549 Table 1 : Volume of water filtered, abundance of *B. truncatus*, molecular prevalence of *Schistosoma* in  
 550 *B. truncatus* populations, specific richness of trematodes that use *B. truncatus* populations as a host  
 551 (other than *Schistosoma*), co-infection rate among infected snails, and average number of reads  
 552 attributed to *Schistosoma* among snails infected by *Schistosoma*, per site.

Site	Volume of water filtered (L)	<i>B. truncatus</i> abundance (DNA copies / litre of filtered water)	Molecular prevalence of <i>Schistosoma</i> in <i>B. truncatus</i>	Trematode richness using <i>B. truncatus</i> as host other than <i>Schistosoma</i>	Rate of co-infections among infected individuals	Average % of <i>Schistosoma</i> reads in <i>B. truncatus</i> individuals infected by <i>Schistosoma</i>
Ndiawara	6.5	78	0,0	4	0.33	00.00
Ouali_Diala	10	41	2,3	3	0.83	34.94
Guia_canal	5	61	23,8	3	1.00	20.67
Dioundou	10	75	0,0	0	NA	00.00
Fonde_Ass	10	57	0,0	1	0.00	00.00
Khodit	5	333	29,4	1	0.20	99.74
Mbane	2.8	104	0,0	0	NA	00.00
Saneinte	3.5	2176	8,3	2	0.25	50.15
Lampsar	18	58	6,3	1	0.25	80.63

553

554 During all the molecular analysis steps, all the negative and positive controls behaved as  
 555 expected. The prevalences of trematodes including that of schistosomes in *B. truncatus* populations,  
 556 assessed from our molecular diagnostic approach, were higher than the prevalences measured by the  
 557 emission method only (Additional\_File\_10\_(Table S3)).

558 Overall the emitting *B. truncatus* infected by *Schistosoma* species and by at least one other  
 559 species of trematode, *Schistosoma* species are shed only when they are dominant in terms of relative  
 560 sequenced reads abundance compared to that of the other co-infecting trematode species  
 561 (Additional\_File\_11\_(Figure\_S5)). Moreover, in all but one case, the haplotype of the trematode  
 562 species emitted corresponds to the most abundant haplotype obtained from NGS sequencing in co-  
 563 infected *B. truncatus* (Figure 3; Additional\_File\_7\_(Table\_S1)).

564 Both the local richness of trematode species exploiting *B. truncatus* population (p-value =  
565 0.029; AIC = 14.9) and the coinfection rate (p-value = 0.020, AIC = 17.4) have a significant negative effect  
566 on *Schistosoma spp.* dominance based on our GLMM models. Conversely, the local abundance of *B.*  
567 *truncatus* positively and significantly affects *Schistosoma spp.* dominance (p-value = 0.047, AIC =20.1).  
568 Based on the comparison of AICs obtained from the three statistical models ran, the model accounting  
569 for the local richness of trematode species exploiting *B. truncatus* population is the best supported  
570 which strengthens the idea that this factor is the most important in explaining *Schistosoma spp.*  
571 dominance. At site level, the co-infection rate among infected snails tended to increase when the total  
572 trematode species richness exploiting the *B. truncatus* population increased, although the correlation  
573 was not significant (Table 1). Conversely, this same co-infection rate tended to decrease when the  
574 abundance of *B. truncatus* increased (Table 1).

575

576

## 577 5. Discussion / Conclusion

578 Understanding the ecological mechanisms that drive the circulation of parasites is primordial  
579 to better identify transmission site, better assess transmission risks and guide strategies to fight against  
580 parasites and the associated diseases while preserving the integrity of the socio-ecosystem health  
581 (28,29). In this context, the ecology of transmission of *Schistosoma* species that are involved in  
582 bilharziasis forms associated to humans and to a lesser extent to animals, and the impact of human  
583 activities on the circulation of these parasites have received considerable attention and particularly so  
584 in the last decade (30,31).

585 The presence and abundance of compatible snail hosts in a given system are determining factors in the  
586 establishment and circulation of *Schistosoma* parasites, particularly as they modulate the rate of  
587 contact between the parasites released into the system and the hosts (i.e. encounter filter; (32,33)).

588 In the present study we theoretically and empirically show that reducing snail host abundance  
589 also hamper the circulation of *S. haematobium* indirectly by promoting snail co-infections with other

590 potentially more competitive trematode species and hence a reduction of *S. haematobium* cercariae  
591 produced by local *B. truncatus* populations. This competition effect on the circulation of *S.*  
592 *haematobium* becomes negligible when *B. truncatus* populations are abundant. In other word, the  
593 size of local snail host populations for parasites of the genus *Schistosoma* may predict the risk of  
594 transmission for definitive vertebrate hosts including humans because it determines not only the  
595 encounter filter, but also modulates the ‘competence’ (*sensu largo*) of the locally established snail hosts  
596 by influencing their probability of being co-infected with other competitive trematode species (i.e.  
597 compatibility filter; (32,33)). This result is based on the generally acknowledged assumption that  
598 *Schistosoma* species are bad to moderate competitors (13,15). Although we could not empirically  
599 assess the hierarchical rank of competitive ability of each trematode detected in *B. truncatus*  
600 populations during our field survey we can expect that at least some of these outcompete or even  
601 predate *S. haematobium*, particularly those known to produce rediae during their intra-mollusc  
602 parasitic stage such as *Petasiger* sp.

603           Coinfections are rarely observed in the field which could suggest that the effect of the resulting  
604 antagonistic interactions between co-occurring parasites could be of relatively weak importance. We  
605 here argue that coinfections are likely to be generally underestimated. In particular, we believe that  
606 traditional techniques to detect trematodes that develop within their snail hosts via dissection or  
607 induced cercarial emission, might lead to an underestimation of coinfection rates. This might be  
608 particularly true when *Schistosoma* species are present in the form of degraded, or even invisible  
609 traces, resulting from competition or predation induced by other trematodes species. In this regard,  
610 high throughput next generation sequencing approaches such as metabarcoding used in this study  
611 appear promising to better assess coinfection rates and overall trematode communities within natural  
612 snail host populations (34). These metabarcoding approaches are the ‘interspecific equivalent’ of the  
613 genotyping approaches that have revealed the initially unsuspected intraspecific diversity of parasites  
614 within their hosts in the past decades (35–37).

615 Our model also points toward the fact that the intensity of such within-snail host competitive  
616 effects on *S. haematobium* cercariae production increases with the number of trematode species using  
617 the targeted *B. truncatus* population. This theoretical result is also supported by our empirical study. It  
618 is interesting to note that the presence of a single highly competitive trematode species at high  
619 abundance at a given transmission site and using a given population of *B. truncatus*, would locally result  
620 in a similar decrease in the amount of cercariae of *S. haematobium* co-occurring at this site. In fact,  
621 biological control strategies based on the dissemination of farmable competitive trematode species  
622 that use snail vectors of parasites of the genus *Schistosoma* at active transmission sites have been  
623 proposed in the past (38). However, this situation, if not artificially maintained, is generally uncommon  
624 *in natura*. Conversely, several studies, including ours, indicate that parasites of the genus *Schistosoma*  
625 naturally cooccur frequently with several trematode species that use *Schistosoma* snail intermediate  
626 hosts in the field (13). Since trematode species composition is determined by the composition of  
627 vertebrate communities locally established either temporary or permanently (39), maintaining  
628 vertebrate host diversity that supports trematode diversity in local snail populations could help to  
629 reduce the transmission of *Schistosoma* species. For this effect to be sustainable over time, the  
630 trematodes released by their vertebrate definitive hosts must complete their entire life cycle locally,  
631 which also implies the maintenance of other compartments of biodiversity, including numerous  
632 vertebrates (e.g. fish, amphibians) and invertebrates (e.g. aquatic insects). Unfortunately, our  
633 ecological knowledge of most trematodes is sorely lacking, and their life cycles are still poorly  
634 documented. Huge works remain to be done to characterise both the fauna involved in supplying  
635 trematodes that interact with species of the genus *Schistosoma* in their intermediate hosts, and the  
636 fauna involved in maintaining the local life cycles of these trematodes. We believe that the newly  
637 available metabarcoding tools such as used in the present study (19,34,40), combined with the  
638 implementation of large and well documented sequence datasets, provide a promising avenue to  
639 characterise trematode life cycles.

640 Our study suggest that maintaining high levels of biodiversity in freshwater aquatic ecosystems  
641 could help reducing the transmission of parasites of the genus *Schistosoma*. Several synergetic effects  
642 of biodiversity could reduce the circulation of these parasites (29). For instance, several organisms  
643 including fish crustaceans and oligochaetes can predate free-living stages of *Schistosoma* parasites and  
644 hence reduce their abundance and therefore the risk of infection for mammals (41). However, the  
645 negative effect of local biodiversity on the circulation of *Schistosoma* species is all the greater when  
646 host snail populations are small. Eradication of snail populations that host *Schistosoma* species is  
647 generally considered as the best alternative to fight against schistosmiasis and is one of the  
648 recommendations of the WHO (42). Although this strategy is theoretically efficient at short term, its  
649 deployment on a large spatial and temporal scale is questionable for several reasons. First, the  
650 molluscicides commonly used and spread into aquatic ecosystems are sometimes poorly accepted by  
651 Human communities using these ecosystems for water supply. Second, the effects of molluscicides on  
652 the overall biodiversity associated with aquatic environments are still poorly understood (43–46).  
653 Finally, while these products are efficient against snail communities established locally, they do not  
654 prevent the recolonization of these species after treatment. In this context, and alternatively to the  
655 application of chemical-based molluscicide, several environment-based strategies aiming at reducing  
656 snail hosts abundance while providing services to local human populations are emerging such as the  
657 introduction of edible predators of snail hosts (e.g. crayfish) or the extraction of specific aquatic plants  
658 that serve as refuge for aquatic snails to produce compost, (47,48). Combined with massive drug  
659 administration campaign in human populations and the application of the WASH protocol (42), these  
660 guided sustainable strategies of reduction or eradication of aquatic snail host populations that  
661 constitute intermediate hosts for *Schistosoma*, generally lead to an important reduction in the rate of  
662 re-infection and prevalence of schistosomiasis in neighbouring human populations (49). We here argue  
663 that the implementation of sustainable strategies to preserve the biodiversity associated with aquatic  
664 ecosystems could be an additional and potentially low-cost means of significantly reducing the  
665 prevalence and intensity of bilharziasis, without necessarily eliminating totally host snail populations.

666 These strategies are in line with the need for concrete applications of the One Health concept,  
667 particularly recently applied in the case of aquatic parasites including schistosomes (50), and the  
668 objectives established by the WHO to reduce the prevalence and intensity of schistosomes below a  
669 threshold below which these diseases can no longer be considered a public health problem (42).

670

671

## 672 6. Références

- 673 1. Gottdenker NL, Streicker DG, Faust CL, Carroll CR. Anthropogenic Land Use Change and Infectious  
674 Diseases: A Review of the Evidence. *EcoHealth*. 1 déc 2014;11(4):619-32.
- 675 2. Jones KE, Patel NG, Levy MA, Storeygard A, Balk D, Gittleman JL, et al. Global trends in emerging  
676 infectious diseases. *Nature*. févr 2008;451(7181):990-3.
- 677 3. White RJ, Razgour O. Emerging zoonotic diseases originating in mammals: a systematic review of  
678 effects of anthropogenic land-use change. *Mammal Rev*. oct 2020;50(4):336-52.
- 679 4. Keesing F, Ostfeld RS. Impacts of biodiversity and biodiversity loss on zoonotic diseases. *Proc Natl  
680 Acad Sci*. 27 avr 2021;118(17):e2023540118.
- 681 5. Bar-On YM, Phillips R, Milo R. The biomass distribution on Earth. *Proc Natl Acad Sci*. 19 juin  
682 2018;115(25):6506-11.
- 683 6. Ceballos G, Ehrlich PR, Barnosky AD, García A, Pringle RM, Palmer TM. Accelerated modern  
684 human-induced species losses: Entering the sixth mass extinction. *Sci Adv*. 19 juin  
685 2015;1(5):e1400253.
- 686 7. Hopkins SR, Fleming-Davies AE, Belden LK, Wojdak JM. Systematic review of modelling  
687 assumptions and empirical evidence: Does parasite transmission increase nonlinearly with host  
688 density? *Methods Ecol Evol*. 2020;11(4):476-86.
- 689 8. Baker RE, Mahmud AS, Miller IF, Rajeev M, Rasambainarivo F, Rice BL, et al. Infectious disease in  
690 an era of global change. *Nat Rev Microbiol*. avr 2022;20(4):193-205.
- 691 9. Civitello DJ, Cohen J, Fatima H, Halstead NT, Liriano J, McMahon TA, et al. Biodiversity inhibits  
692 parasites: Broad evidence for the dilution effect. *Proc Natl Acad Sci*. 14 juill  
693 2015;112(28):8667-71.
- 694 10. Halsey S. Defuse the dilution effect debate. *Nat Ecol Evol*. févr 2019;3(2):145-6.
- 695 11. McCallum HI. Lose biodiversity, gain disease. *Proc Natl Acad Sci*. 14 juill 2015;112(28):8523-4.
- 696 12. Wood CL, Lafferty KD, DeLeo G, Young HS, Hudson PJ, Kuris AM. Does biodiversity protect humans  
697 against infectious disease? *Ecology*. 2014;95(4):817-32.

- 698 13. Laidemitt MR, Anderson LC, Wearing HJ, Mutuku MW, Mkoji GM, Loker ES. Antagonism between  
699 parasites within snail hosts impacts the transmission of human schistosomiasis. *eLife*. 17 déc  
700 2019;8:e50095.
- 701 14. Jourdane J, Mounkassa JB, Imbert-Establet D. Influence of intramolluscan larval stages of  
702 *Echinostoma liei* on the infectivity of *Schistosoma mansoni* cercariae. *J Helminthol*. mars  
703 1990;64(1):71-4.
- 704 15. Kuris AM, Lafferty KD. COMMUNITY STRUCTURE: Larval Trematodes in Snail Hosts. *Annu Rev Ecol*  
705 *Syst*. 1994;25(1):189-217.
- 706 16. Laidemitt MR, Gleichsner AM, Ingram CD, Gay SD, Reinhart EM, Mutuku MW, et al. Host  
707 preference of field-derived *Schistosoma mansoni* is influenced by snail host compatibility and  
708 infection status. *Ecosphere*. 2022;13(4):e4004.
- 709 17. Leger E, Webster JP. Hybridizations within the Genus *Schistosoma*: implications for evolution,  
710 epidemiology and control. *Parasitology*. janv 2017;144(1):65-80.
- 711 18. Senghor B, Mathieu-Begné E, Rey O, Doucouré S, Sow D, Diop B, et al. Urogenital schistosomiasis  
712 in three different water access in the Senegal river basin: prevalence and monitoring praziquantel  
713 efficacy and re-infection levels. *BMC Infect Dis*. 29 déc 2022;22(1):968.
- 714 19. Douchet P, Boissier J, Mulero S, Ferté H, Doberva M, Allienne J, et al. Make visible the invisible:  
715 Optimized development of an environmental DNA metabarcoding tool for the characterization of  
716 trematode parasitic communities. *Environ DNA*. mai 2022;4(3):627-41.
- 717 20. Blin M, Senghor B, Boissier J, Mulero S, Rey O, Portela J. Development of environmental loop-  
718 mediated isothermal amplification (eLAMP) diagnostic tool for *Bulinus truncatus* field detection.  
719 *Parasit Vectors*. 28 févr 2023;16(1):78.
- 720 21. Mulero S, Boissier J, Allienne JF, Quilichini Y, Foata J, Pointier JP, et al. Environmental DNA for  
721 detecting *Bulinus truncatus*: A new environmental surveillance tool for schistosomiasis  
722 emergence risk assessment. *Environ DNA*. 2020;2(2):161-74.
- 723 22. Escudié F, Auer L, Bernard M, Mariadassou M, Cauquil L, Vidal K, et al. FROGS: Find, Rapidly, OTUs  
724 with Galaxy Solution. *Bioinformatics*. 15 avr 2018;34(8):1287-94.
- 725 23. Mahé F, Rognes T, Quince C, Vargas C de, Dunthorn M. Swarm: robust and fast clustering method  
726 for amplicon-based studies. *PeerJ*. 25 sept 2014;2:e593.
- 727 24. Rognes T, Flouri T, Nichols B, Quince C, Mahé F. VSEARCH: a versatile open source tool for  
728 metagenomics. *PeerJ*. 18 oct 2016;4:e2584.
- 729 25. Madeira F, Park Y mi, Lee J, Buso N, Gur T, Madhusoodanan N, et al. The EMBL-EBI search and  
730 sequence analysis tools APIs in 2019. *Nucleic Acids Res*. 2 juill 2019;47(W1):W636-41.
- 731 26. Waterhouse AM, Procter JB, Martin DMA, Clamp M, Barton GJ. Jalview Version 2—a multiple  
732 sequence alignment editor and analysis workbench. *Bioinformatics*. 1 mai 2009;25(9):1189-91.
- 733 27. McMurdie PJ. joey711/phyloseq [Internet]. 2024 [cité 18 mars 2024]. Disponible sur:  
734 <https://github.com/joey711/phyloseq>



- 735 28. De Garine-Wichatitsky M, Binot A, Ward J, Caron A, Perrotton A, Ross H, et al. "Health in" and  
736 "Health of" Social-Ecological Systems: A Practical Framework for the Management of Healthy and  
737 Resilient Agricultural and Natural Ecosystems. *Front Public Health* [Internet]. 2021 [cité 24 août  
738 2023];8. Disponible sur: <https://www.frontiersin.org/articles/10.3389/fpubh.2020.616328>
- 739 29. Douchet P, Gourbal B, Loker ES, Rey O. *Schistosoma* transmission: scaling-up competence from  
740 hosts to ecosystems. *Trends Parasitol*. juill 2023;39(7):563-74.
- 741 30. Hoover CM, Rumschlag SL, Strgar L, Arakala A, Gambhir M, Leo GA de, et al. Effects of  
742 agrochemical pollution on schistosomiasis transmission: a systematic review and modelling  
743 analysis. *Lancet Planet Health*. 1 juill 2020;4(7):e280-91.
- 744 31. Shaikh N, Rahman-Shepherd A, Dar O. Schistosomiasis in the Senegal River basin. *Lancet Planet*  
745 *Health*. 1 mai 2018;2:S27.
- 746 32. Combes C. *Parasitism: The Ecology and Evolution of Intimate Interactions*. University of Chicago  
747 Press; 2001. 743 p.
- 748 33. Kincaid-Smith J, Rey O, Toulza E, Berry A, Boissier J. Emerging Schistosomiasis in Europe: A Need  
749 to Quantify the Risks. *Trends Parasitol*. 1 août 2017;33(8):600-9.
- 750 34. Hammoud C, Mulero S, Van Bocxlaer B, Boissier J, Verschuren D, Albrecht C, et al. Simultaneous  
751 genotyping of snails and infecting trematode parasites using high-throughput amplicon  
752 sequencing. *Mol Ecol Resour*. 2022;22(2):567-86.
- 753 35. Criscione CD, Poulin R, Blouin MS. Molecular ecology of parasites: elucidating ecological and  
754 microevolutionary processes. *Mol Ecol*. 2005;14(8):2247-57.
- 755 36. Dabo A, Durand P, Morand S, Diakite M, Languard J, Imbert-Establet D, et al. Distribution and  
756 genetic diversity of *Schistosoma haematobium* within its bulinid intermediate hosts in Mali. *Acta*  
757 *Trop*. 24 juin 1997;66(1):15-26.
- 758 37. Theron A, Sire C, Rognon A, Prugnolle F, Durand P. Molecular ecology of *Schistosoma mansoni*  
759 transmission inferred from the genetic composition of larval and adult infrapopulations within  
760 intermediate and definitive hosts. *Parasitology*. nov 2004;129(5):571-85.
- 761 38. Combes C. Trematodes: antagonism between species and sterilizing effects on snails in biological  
762 control. *Parasitology*. avr 1982;84(4):151-75.
- 763 39. Hechinger RF, Lafferty KD. Host diversity begets parasite diversity: bird final hosts and trematodes  
764 in snail intermediate hosts. *Proc R Soc B Biol Sci*. 20 mai 2005;272(1567):1059-66.
- 765 40. Thomas LJ, Milotic M, Vaux F, Poulin R. Lurking in the water: testing eDNA metabarcoding as a  
766 tool for ecosystem-wide parasite detection. *Parasitology*. févr 2022;149(2):261-9.
- 767 41. Koprivnikar J, Thieltges DW, Johnson PTJ. Consumption of trematode parasite infectious stages:  
768 from conceptual synthesis to future research agenda. *J Helminthol*. janv 2023;97:e33.
- 769 42. WHO WH. Ending the neglect to attain the sustainable development goals: a road map for  
770 neglected tropical diseases 2021–2030. 2020 [cité 7 oct 2023]; Disponible sur:  
771 [https://policycommons.net/artifacts/538380/ending-the-neglect-to-attain-the-sustainable-](https://policycommons.net/artifacts/538380/ending-the-neglect-to-attain-the-sustainable-development-goals/1515029/)  
772 [development-goals/1515029/](https://policycommons.net/artifacts/538380/ending-the-neglect-to-attain-the-sustainable-development-goals/1515029/)

- 773 43. Andrews P, Thyssen J, Lorke D. The biology and toxicology of molluscicides, bayluscide. *Pharmacol*  
774 *Ther.* 1 janv 1982;19(2):245-95.
- 775 44. Dawson VK. Environmental Fate and Effects of the Lampricide Bayluscide: a Review. *J Gt Lakes*  
776 *Res.* 1 janv 2003;29:475-92.
- 777 45. King CH, Sutherland LJ, Bertsch D. Systematic Review and Meta-analysis of the Impact of  
778 Chemical-Based Mollusciciding for Control of *Schistosoma mansoni* and *S. haematobium*  
779 Transmission. *PLoS Negl Trop Dis.* 28 déc 2015;9(12):e0004290.
- 780 46. Takougang I, Meli J, Wabo Poné J, Angwafo F. Community acceptability of the use of low-dose  
781 niclosamide (Bayluscide®), as a molluscicide in the control of human schistosomiasis in Sahelian  
782 Cameroon. *Ann Trop Med Parasitol.* 1 sept 2007;101(6):479-86.
- 783 47. Rohr JR, Sack A, Bakhoum S, Barrett CB, Lopez-Carr D, Chamberlin AJ, et al. A planetary health  
784 innovation for disease, food and water challenges in Africa. *Nature.* juill 2023;619(7971):782-7.
- 785 48. Sokolow SH, Huttinger E, Jouanard N, Hsieh MH, Lafferty KD, Kuris AM, et al. Reduced  
786 transmission of human schistosomiasis after restoration of a native river prawn that preys on the  
787 snail intermediate host. *Proc Natl Acad Sci.* 4 août 2015;112(31):9650-5.
- 788 49. Sokolow SH, Wood CL, Jones IJ, Lafferty KD, Kuris AM, Hsieh MH, et al. To Reduce the Global  
789 Burden of Human Schistosomiasis, Use 'Old Fashioned' Snail Control. *Trends Parasitol.* 1 janv  
790 2018;34(1):23-40.
- 791 50. Selbach C, Mouritsen KN, Poulin R, Sures B, Smit NJ. Bridging the gap: aquatic parasites in the  
792 One Health concept. *Trends Parasitol.* 1 févr 2022;38(2):109-11.

793

794

## 795 [Figures in main text](#)

796 Figure 1: Satellite map of the studied area in Northern Senegal.

797 This map indicates the location of the 9 targeted sites (black dots) and the name of the nearby 9

798 villages associated to these *S. haematobium* transmission sites.

799

800 Figure 2 : Co-infection ratio, *Schistosoma* prevalence, and *Schistosoma* cercariae ratio, for three values  
801 of the carrying capacity.

802 The co-infection ratio is the ratio between the number of co-infected *B. truncatus* and the total number  
803 of infected *B. truncatus*. The *Schistosoma* cercariae ratio is the ratio between the number of *Schistosoma*  
804 cercariae and the total number of cercariae. The dashed purple line indicates the *Schistosoma* cercariae  
805 ratio in case the *Schistosoma* shedding rate is the same as for the other trematode species. The reduction

806 of the *Schistosoma* cercariae ratio (difference between full and dashed purple line) is due to coinfections  
807 and to the inferior competitiveness of *Schistosoma*. The carrying capacity  $K$  differs by factors of 10 of the  
808 snail population.

809

810 Figure 3: Relative abundance of trematode species in percentages of obtained sequenced reads  
811 exploiting infected *B. truncatus* individual.

812 Infected snails (in columns) are grouped by site. The black dots correspond to the species of trematode  
813 emitted by the emitting snails (confirmed by SANGER sequencing and BLAST assignment).

814

815

## 816 7. Additional files

817 File name : Additional\_File\_1\_(Figure\_S1)

818 File format : .png

819 Title and description of the data : Equilibrium changes of density of miracidia, cercariae, susceptible  
820 and infected snails, as a function of the carrying capacity ( $K$ ) of the snail population in the case of one  
821 trematode species infect the snail population.

822

823 File name : Additional\_File\_2\_(Figure\_S2)

824 File format : .png

825 Title and description of the data : Equilibrium changes of density of total miracidia and total cercariae  
826 of two trematodes species including one with a lowest competitive capacity (i.e., *Schistosoma*), and of  
827 density of susceptible and infected snails, as a function of the carrying capacity  $K$  of the snail population.

828

829 File name : Additional\_File\_3\_(Figure\_S3)

830 File format : .png

831 Title and description of the data : Equilibrium changes of co-infection ratio and *Schistosoma* cercariae  
832 density ratio as a function of the carrying capacity ( $K$ ) of the snail population in the case of two  
833 trematodes species infecting the snail population. Note that without co-infection the ratio of *Schistosoma*

834 cercariae would be equal to 1/2. The deviation observed here is due to, and increases with, the co-  
835 infection ratio.

836

837 File name : Additional\_File\_4\_(Supplementary\_material)

838 File format : .doc

839 Title and description of the data : Supplementary\_material providing an in-depth description of the  
840 model equations and simulations

841

842 File name : Additional\_File\_5\_divpara\_main.m

843 File format : MatLab (.m) <https://fr.mathworks.com/products/matlab.html>

844 Title and description of the data : MatLab script to generate Figure 2

845

846 File name : Additional\_File\_6\_divpara\_rhs.m

847 File format : MatLab (.m) <https://fr.mathworks.com/products/matlab.html>

848 Title and description of the data : MatLab functions to evaluate the right-hand side of the model  
849 equations

850

851 File name : Additional\_File\_7\_(Table S1)

852 File format : .xls

853 Title and description of the data : OTUs table assigned as trematodes of *B truncatus* from the  
854 experimental infection positive to the trematode diagnostic

855

856 File name : Additional\_File\_8\_(Figure\_S4)

857 File format : .png

858 Title and description of the data : Number of *B. truncatus* individuals non infected, and infected by one  
859 to 4 parasites species. Observed data are shown as bars. The negative binomial theoretical distribution  
860 is represented by the black dots. The Chi2 test shows no statistical difference between the observed  
861 distribution and the theoretical distribution suggesting a parasites aggregation in host populations (p-  
862 value = 0.9985).

863

864 File name : Additional\_File\_9\_(Table S2)

865 File format : .xls

866 Title and description of the data : OTUs assigned as trematodes found in water filtrations and in *B*  
867 *truncatus* populations

868

869

870 File name : Additional\_File\_10\_(Table S3)

871 File format : .xls

872 Title and description of the data : Prevalence of *Schistosoma* and trematodes in the different  
873 populations of *B. truncatus*

874

875 File name : Additional\_File\_11\_(Figure S5)

876 File format : .png

877 Title and description of the data : Cercariae emission of *S. haematobium* or *S. bovis* as a function of  
878 their relative abundance in case of co-infection with one or more other trematode species. Only *B.*  
879 *truncatus* snails emitters infected by one species of *Schistosoma* and by at least one other species of  
880 trematode were taken into account in this analysis (i.e. 14 snails). Intra-mollusc parasitic stages and  
881 cercariae of schistosomes are illustrated in red. Purple represents the intra-mollusc parasitic stages and  
882 cercariae of other co-infecting trematode species.



Ouali Diala

Fondé ass

Dioundou

Khodit

Ndiawara

Guia

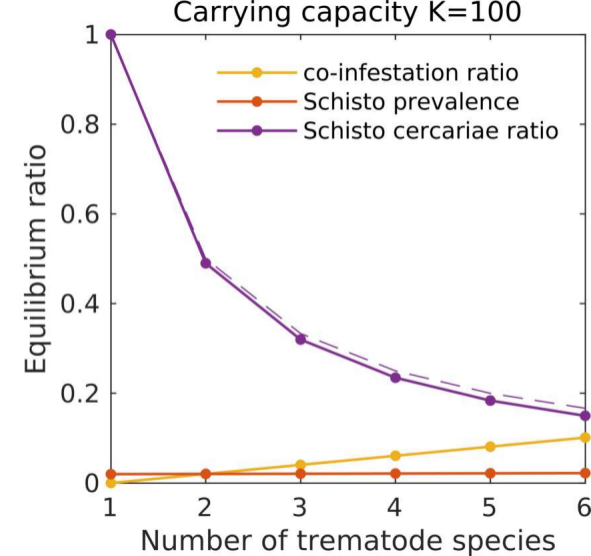
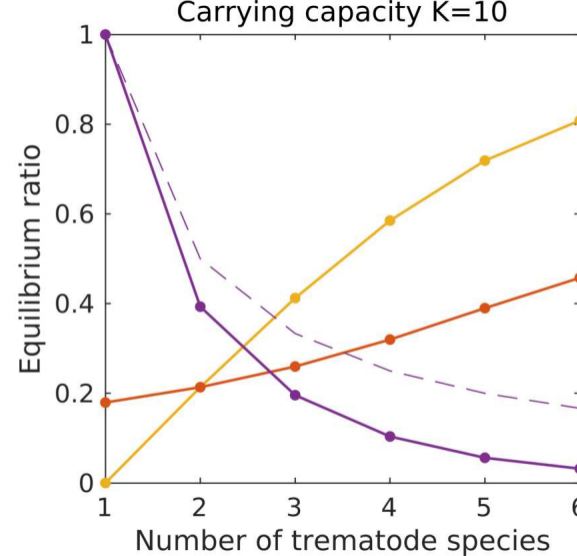
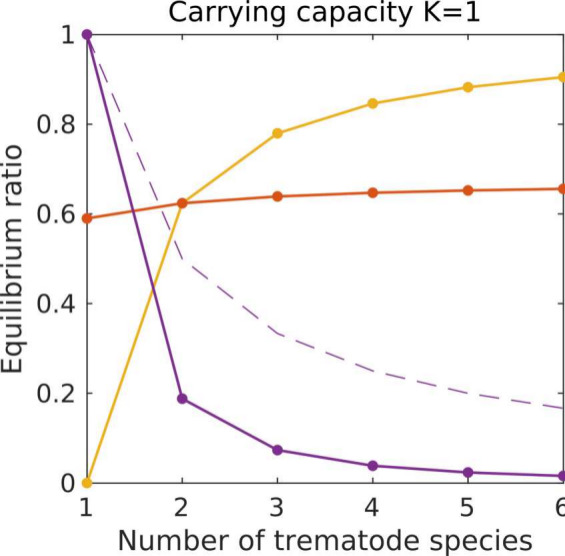
Mbane

Saninte

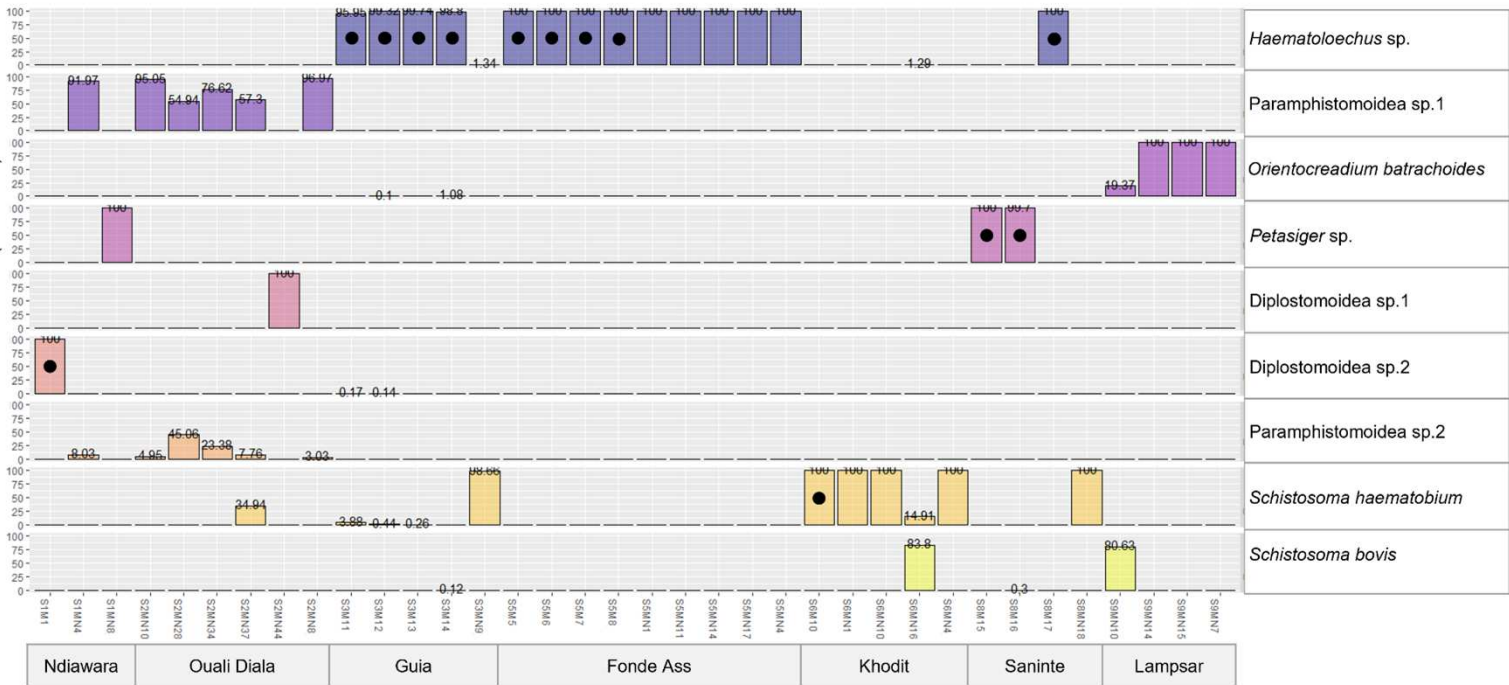
Lampsar



20 km



Relative abundance (in reads %)



Ndiawara

Ouali Diala

Guia

Fonde Ass

Khodit

Saninte

Lampsar



# Supplementary Files

This is a list of supplementary files associated with this preprint. Click to download.

- [AdditionalFile1FigureS1.png](#)
- [AdditionalFile2FigureS2.png](#)
- [AdditionalFile3FigureS3.png](#)
- [AdditionalFile4Supplementarymaterial.docx](#)
- [AdditionalFile5divparamain.m](#)
- [AdditionalFile6divpararhs.m](#)
- [AdditionalFile7TableS1.xlsx](#)
- [AdditionalFile8FigureS4.png](#)
- [AdditionalFile9TableS2.xlsx](#)
- [AdditionalFile10TableS3.xlsx](#)
- [AdditionalFile11FigureS5.png](#)